On the nature of heavy-fermion behaviour and high-field dilatation experiments

Wyder, U.

Publication date
2003

Chapter 4
MEASURING TECHNIQUES

Dilatation experiments were carried out using a technique that is frequently mentioned in literature (e.g. [1][2]). It is basically an electro-mechanical technique where a change in the length of the sample is transferred into a change in spacing between two parallel capacitance plates. It is the change in this capacitance which is measured. We adapted the design of A. de Visser ([1]) for our purposes in high magnetic fields. The used design is depicted below.

By means of the spring system, indicated as number (4) in Fig.1, a plate of the capacitor, indicated as number (2) is mechanically fixed to the sample. As the sample changes its length (due to a change in magnetic field or temperature) this plate, that is connected to the sample, (number (2)) moves with respect to the fixed plate (number (1)). The fixed plate, the plate that is connected to the sample, and the sample with its screws and spring system are all electrically isolated from the housing of the cell. This housing is made from the same copper as the rest of the cell.

The change of capacitance as a result of the change in spacing between the two capacitance plates (d) is recorded. The capacitance, C, is given as:

$$C = \frac{\epsilon A}{d}, \tag{4.1}$$

where $\epsilon = \epsilon_0 \times \epsilon_r$ represents the dielectric constant of the medium between the plates and where A is the area of the plates. From the change in capacitance, C, the change in spacing between the plates, d, can be deduced and hence the length change of the sample can be determined.

As the relative length changes measured are small, i.e. in the order of 10^{-8}, the capacitance has to be measured sensitively. In which case stray capacitances between upper plate and environment and lower plate and environment start to be of importance. A three-terminal method is employed.We were able to measure the capacitance up to an accuracy of $\approx 10^{-8}$ pF. Typically for our experimental arrangement is a capacitance in the order of $C \approx 10^{-11}$ F and $\epsilon A \approx 10^{-15}$ mF. As a result a sensitivity of 5×10^{-2}Å can be reached.

To determine actual length changes of the sample itself (for changing temperatures and magnetic fields) from the measured capacitance changes, the cell first has to be calibrated. We have to take care of two additional facts. The thermal-expansion

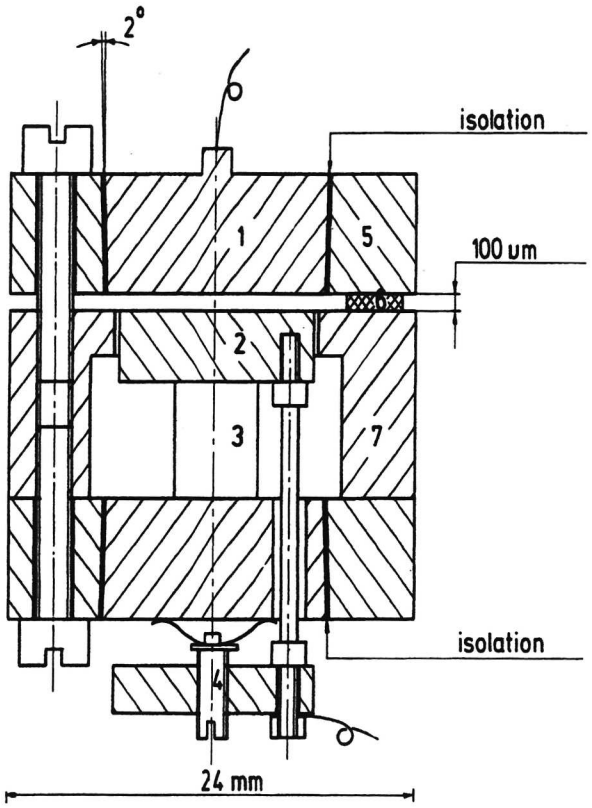

Figure 1 Used capacitance cell; (1) upper plate; (2) lower plate; (3) sample; (4) screw and springs; (5) guard ring upper plate; (6) copper foil (not on scale); (7) guard ring. The lower capacitance plate is positioned by three rods (only one is shown), that are lead through the bottom of the cell. At the lower end the rods are connected to a flat disk, which is positioned by a screw/spring mechanism, clamping the sample between the lower capacitance plate and the bottom of the cell.

and magnetostriction of the cell itself has to be accounted for. It is the result of it being a mechanical device (e.g. tensions in the system -spring system etc.-) and the fact that the cell is made of a material which has a thermal expansion of its own. Furthermore the proportionality constant ϵA has to be determined.

The influence of the dielectric constant of the small amount of helium gas, present in the gap could be neglected. Therefore $\epsilon = \epsilon_0 \epsilon_r = \epsilon_0$. A is determined by measuring the capacitances for different spacer distances at room temperature. The relevant surfaces of the plates are shaped plan parallel within 1 μm by means of spark erosion. The gap distance is provided by placing three copper foils between the guard rings of the upper and lower plates. By the above method, the effective area of the capacitance plates is determined to be equal to:

$$\epsilon A = 9.52 \times 10^{-16} \text{ mF}.$$

The uncertainty in the determination of this value puts an accuracy limit of $\pm 3\%$ on the absolute value of the experimental data. In the actual measuring setup a spacing of abouth 100 μm is used.

The cell is made out of OFHC (Oxygen Free High Conductivity) copper. This material also displays an, although small, non-zero thermal expansion and magnetostriction. For all intent and purposes, the magnetostriction of this copper material, in the temperature field region we are interested in, can be neglected. It is the thermal expansion coefficient which is our major concern here.

The coefficient of the linear thermal expansion is defined as:

$$\alpha \equiv -\frac{1}{L}\frac{\Delta L}{\Delta T}. \tag{4.2}$$

It has been measured in a discontinuous fashion, i.e. by step-wise heating. The value of α for the sample is then calculated from:

$$\alpha_{\text{sample}} = -\frac{1}{L}\frac{\Delta d}{\Delta T}_{\text{cell+sample}} + \frac{1}{L}\frac{\Delta d}{\Delta T}_{\text{cell+Cu sample}} + \alpha_{\text{Cu}} \tag{4.3}$$

The second term on the right is the length change as measured by the cell where the sample is replaced by an equally sized sample made from the same Cu as the cell. The third term on the right, α_{Cu}, is there to compensate for the thermal expansion of the copper ([3]). For this the data of Kroeger and Swenson have been used. $\frac{1}{L}\frac{\Delta d}{\Delta T}_{\text{cell+Cu sample}} + \alpha_{\text{Cu}}$ compensates for the measured thermal expansion as a result of the cell itself. Copper is used as a reference material, as it is the material the cell is made of and as sufficiently accurate thermal expansion data are available.

Typically, the cell effect ranges from $\frac{\Delta d}{\Delta T} \approx -5$ (Å/K) to almost 0 (Å/K) in the first 20 kelvin. It are these first 20 K which form for us the interesting temperature region. In the next 80 kelvin it reaches to -10 (Å/K).

From the point of view of a small enough thermal-expansion coefficient and no magnetostriction at low temperatures, another suitable material to construct capacitance cells from is Silicon. A different cell-layout could be a design where the plates are arranged as a wedge with the sample in between. Such an arrangement could handle smaller samples. In our case the samples must be in the order of $5 \times 5 \times 5$ mm^3. A disadvantage of such a design is that it has in general a larger cell effect.

The dilatation experiments have been performed in the high-magnetic field installation of the Nijmegen High Field Magnet Laboratory ([4][5][6]. In our experiments we made use of a Bitter-type magnet for the "low-field" experiments (up to 17 T), while for the high-field experiments (up to 24.5 T) a hybrid magnet was used. This hybrid magnet consists of a large superconducting magnet surrounding a water-cooled Bitter-type insert magnet. The insert can generate a maximum field of 17 T while the superconducting coil is operated at 8 T. A nice feature of the design as it exists in Nijmegen is the relatively large bore available for experiments (our cell is relatively bulky). Above the magnet a cryostat is placed which has a long tail reaching into the bore of the magnet. The dilatation insert is placed in the tail of the cryostat, with the sample at the centre of the magnet.

The cell can be mounted in various orientations allowing us to vary both the crystal axis along which the dilatation is measured as well as the crystal axis along which the field is applied. In most of our experiments on the $U(Pt_{1-x}Pd_x)_3$ compounds the field is applied along the a-axis. This is done to avoid torque effects on the sample as a result of the particular magnetization of these compounds in fields ($0 \leq B \leq 24.5$ T) and temperatures ($1.2 \leq T \leq 20$ K).

The cell with its wiring etc. is placed in a vacuum chamber fitting into the long tail of the cryostat. All wires are thermally anchored to a cold finger at the bath of the cryostat. The length of the tail of the cryostat and the use of the wiring material ensure a negligible heat loss along the wires.

The use of such fields imposes some restrictions. Noise is generated, both mechanically and magnetically. There is a restriction both in space (the capacitance cell has to fit into the magnet) and time.

The energy of the magnets is provided by two 3 MW power supplies. The cooling system of the resistive magnets and the power supply consist of a primary system, using an ice bunker containing 150 tons of ice and two identical secondary cooling systems which are filled with de-ionized water. The cooling capacity provided by the ice bunker is approximately 18 MWh, which corresponds to 3 hours continuous operation at maximum power. This often was a limiting factor in particular where thermal-expansion experiments were concerned (typically 1 hour for a run from 1.5-20 K). Measurements had to be performed as fast and as accurate as possible. We will come back to this point in a moment.

The mechanical noise was suppressed by mounting the cryostat onto rubber dampers. The cooling water system causes also vibrations in the position of the

cryostat with respect to the magnet. These are irregular and with occasional shocks. These can cause the sample to move with respect to the field, which is not perfectly homogeneous. The homogeneity in 1 cm (perpendicular to the field direction) ranges from 1×10^{-5} to 1×10^{-3} for the Bitter magnet, and 3×10^{-3} for the hybrid system.

The stability of the magnetic field is governed by the stability of the power supply. This has a current stability of 0.01 % for short intervals (1 hour) and 0.1 % for long intervals (10 hours). These variations are not of importance for our measurements.

The lowest regulated field available is 0.5 T. Switching the power supply on and off usually causes enough of a disturbance to affect our experiments. This implies that for purposes of comparisons we often had to use the data obtained at 0.5 T instead of the 0 T data.

Always either the field or the temperature was kept fixed while the other was varied. In experiments where the temperature was varied, the temperature was measured by RuO_2 thermometers. RuO_2 thermometers have a considerable magnetoresistance ([7][8][9]). When the magnetic field was swept a carbon glass capacitance thermometer is used to regulate temperature. Such a thermometer has hardly any magnetoresistance effect. On the other hand, it does not reproduce its initial value in a temperature cycle. RuO_2 thermometers were calibrated as function of field and temperature. A grid was formed by measured resistance curves along fixed temperature and fixed field lines covering the region $1.2 \leq T \leq 25$ K and $0 \leq B \leq 24$ K. This grid was fitted by a two dimensional spline.

To avoid too much eddy-current heating during a field sweep, a small amount of Helium exchange gas had to be let into the vacuum chamber. As the helium bath in the cryostat was at 4.2 K the amount of exchange gas introduced was just sufficient to cool the cell from 100 K to 4.2 K in over two hours. After that the bath was pumped to 1.4 K, the base temperature for all our experiments.

Magnetostriction curves were obtained by continuously recording data while the magnetic field was swept with a constant (slow) rate. Temperature was kept constant by means of a PID regulation circuit using the capacitance thermometer. The by the field sweep introduced eddy-current could than be treated as simply an extra heating current.

To ensure that no temperature gradients are introduced during field sweeps or temperature variations, two (almost) identical RuO_2 thermometers were mounted onto the cell. We had the luck to have two such thermometers available, otherwise we just would have cut an existing RuO_2 thermometer lengthwise into two parts. Care was taken that both thermometers were as close as possible to the sample and the plates. Only when the temperature change (as a function of time) of both sensors as well as the temperature difference between both sensors attained a prefixed value, a data point was measured. To ensure consistency and for purposes of speed this was controlled by a computer program

This program also controlled the increments in temperature. Two options

were available. A PID regulation could be used to reach a preset temperature or a fixed increment in heater current could be given after which the program waited until the desired accuracy was reached. It turned out that for the case of the pumped helium bath and the low-temperature region (below ≈ 10 K), the second method was faster while for the higher temperature region and an un-pumped helium bath the first method was faster. They do not differ in measuring accuracy.

Again, to avoid temperature gradients over the cell also two heaters were used.

A reason to be so aware of temperature gradients is the fact that the fit of our system into the cryostat is relatively snug. Radial gradients over the cell towards the cold wall of the vacuum chamber and the tail of the cryostat should be avoided.

Basically, the thermal expansion is the (normalized) derivative of the length (L) as function of the temperature (T). To increase measuring accuracy instead of two points, three points were used to determine the derivative.

Assume, one knows the length of the sample at two different temperatures, say T_1 and T_2; how does one determine the derivative of the length, $\frac{\partial L(T)}{\partial T}$ for a temperature T, $T_1 \leq T \leq T_2$? One can make two Taylor expansions:

$$L(T_1) = L(T) + (T_1 - T)\frac{\partial L(T)}{\partial T} + \frac{1}{2}(T_1 - T)^2 \frac{\partial^2 L(T)}{\partial T^2} + ..., \quad (4.4)$$

$$L(T_2) = L(T) + (T_2 - T)\frac{\partial L(T)}{\partial T} + \frac{1}{2}(T_2 - T)^2 \frac{\partial^2 L(T)}{\partial T^2} + ... \quad (4.5)$$

Hence:

$$L(T_2) - L(T_1) = (T_2 - T_1)\frac{\partial L(T)}{\partial T} + \frac{1}{2}\left(T_2^2 - T_1^2 - 2T(T_2 - T_1)\right)\frac{\partial^2 L(T)}{\partial T^2} + ..., \quad (4.6)$$

$$\frac{\partial L(T)}{\partial T} = \frac{L(T_2) - L(T_1)}{(T_2 - T_1)} - \frac{\frac{1}{2}\left(T_2^2 - T_1^2 - 2T(T_2 - T_1)\right)}{(T_2 - T_1)}\frac{\partial^2 L(T)}{\partial T^2} - \quad (4.7)$$

Approximately $\frac{\partial L(T)}{\partial T} \approx \frac{L(T_2) - L(T_1)}{(T_2 - T_1)}$ holds. The error made will be in the order of $\frac{\frac{1}{2}\left(T_2^2 - T_1^2 - 2T(T_2 - T_1)\right)}{(T_2 - T_1)}\frac{\partial^2 L(\epsilon)}{\partial T^2}$ with $T_1 \leq \epsilon \leq T_2$. The temperature to which this derivative should be assigned is determined by minimizing the error. To minimize this error choose, T so that $\frac{\frac{1}{2}\left(T_2^2 - T_1^2 - 2T(T_2 - T_1)\right)}{(T_2 - T_1)}$ is at its minimum; that is when:

$$T = \frac{T_2 - T_1}{T_2 + T_1}. \quad (4.8)$$

Here, we made use of the fact that $L(T)$ is a smooth function, so that as its derivatives get of higher order, they only get smaller. The accuracy of the method

is increased by using three points instead of 2; say $T_1 < T_2 < T_3$. We introduce the following notation:

$$T_1 = T + h_1, \tag{4.9}$$
$$T_2 = T + h_2, \tag{4.10}$$
$$T_3 = T + h_3 \tag{4.11}$$

then:

$$L(T_1) = L(T) + h_1\frac{\partial L(T)}{\partial T} + \frac{1}{2}h_1^2\frac{\partial^2 L(T)}{\partial T^2} + \frac{1}{6}h_1^3\frac{\partial^3 L(T)}{\partial T^3} + ..., \tag{4.12}$$
$$L(T_2) = L(T) + h_2\frac{\partial L(T)}{\partial T} + \frac{1}{2}h_2^2\frac{\partial^2 L(T)}{\partial T^2} + \frac{1}{6}h_2^3\frac{\partial^3 L(T)}{\partial T^3} + ..., \tag{4.13}$$
$$L(T_2) = L(T) + h_3\frac{\partial L(T)}{\partial T} + \frac{1}{2}h_3^2\frac{\partial^2 L(T)}{\partial T^2} + \frac{1}{6}h_3^3\frac{\partial^3 L(T)}{\partial T^3} + ... \tag{4.14}$$

Now we obtain:

$$L(T_1) - L(T_2) = (h_1 - h_2)\frac{\partial L(T)}{\partial T} + \frac{(h_1^2 - h_2^2)}{2}\frac{\partial^2 L(T)}{\partial T^2} + \frac{(h_1^3 - h_2^3)}{6}\frac{\partial^3 L(T)}{\partial T^3} + ..., \tag{4.15}$$
$$L(T_2) - L(T_3) = (h_2 - h_3)\frac{\partial L(T)}{\partial T} + \frac{(h_2^2 - h_3^2)}{2}\frac{\partial^2 L(T)}{\partial T^2} + \frac{(h_2^3 - h_3^3)}{6}\frac{\partial^3 L(T)}{\partial T^3} + ... \tag{4.16}$$

Eliminating the second order derivative, $\frac{\partial^2 L(T)}{\partial T^2}$, from this set of equations results in:

$$\frac{\partial L(T)}{\partial T} = \frac{\left[\frac{(h_1-h_2)(L(T_1)-L(T_2))}{h_1^2-h_2^2} - \frac{(h_2-h_3)(L(T_2)-L(T_3))}{h_2^2-h_3^2}\right]}{\left[\frac{(h_1-h_2)}{h_1^2-h_2^2} - \frac{(h_2-h_3)}{h_2^2-h_3^2}\right]} - \frac{3}{2}R(h_1,h_2,h_3)\frac{\partial^3 L(T)}{\partial T^3} + ... \tag{4.17}$$

with:

$$R(h_1,h_2,h_3) = \frac{\frac{h_1^3-h_2^3}{3(h_1^2-h_2^2)} - \frac{h_1^3-h_2^3}{3(h_1^2-h_2^2)}}{\frac{2(h_1-h_2)}{(h_1^2-h_2^2)} - \frac{2(h_1-h_2)}{(h_1^2-h_2^2)}}, \tag{4.18}$$

$$= \frac{(T_1^3 - T_3^3 - 3T(T_1^2 - T_3^2) - 3T^2(T_1 - T_3))(T_2^2 - T_3^2 - 2T(T_2 - T_3))}{(T_1 - T_2)(T_2^2 - T_3^2 - 2T(T_2 - T_3)) - (T_2 - T_3)(T_1^2 - T_2^2 - 2T(T_1 - T_2))} -$$
$$\frac{(T_2^3 - T_3^3 - 3T(T_2^2 - T_3^2) - 3T^2(T_2 - T_3))(T_1^2 - T_3^2 - 2T(T_1 - T_3))}{(T_1 - T_2)(T_2^2 - T_3^2 - 2T(T_2 - T_3)) - (T_2 - T_3)(T_1^2 - T_2^2 - 2T(T_1 - T_2))}.$$

Setting:

$$\frac{\partial L(T)}{\partial T} \approx \frac{\left[\frac{(h_1-h_2)(L(T_1)-L(T_2))}{h_1^2-h_2^2} - \frac{(h_2-h_3)(L(T_2)-L(T_3))}{h_2^2-h_3^2}\right]}{\left[\frac{(h_1-h_2)}{h_1^2-h_2^2} - \frac{(h_2-h_3)}{h_2^2-h_3^2}\right]}, \tag{4.19}$$

then its error will be in the order of $R\frac{\partial^3 L(\epsilon)}{\partial T^3}$ with $T_1 \leq \epsilon \leq T_3$. We choose T so that $R = 0$. This is an equation which can be solved. It has three solutions, two of which have a imaginary contribution and can, therefore, be omitted, whiles the third term is real. It is this solution we are interested in (see footnote). The result is an expression which is for humans not straightforwardly transparent, but a computer has much less difficulties with it. With the help of this expression we determine T. For the so found T always $T_1 \leq T \leq T_2$ holds. Once T is determined we determine h_1, h_2 and h_3. With the help of Eq. 4.19 we can determine the derivative itself. Consider, for a moment, only the situation where the temperature is increased. When the next temperature is measured, this will be $L(T_3)$ while $L(T_2)$ will turn into$L(T_1)$ and $L(T_3)$ will turn into $L(T_2)$. For a fixed measuring accuracy of the temperature and capacitance this method is considerably more accurate as a methods based on Eq. 4.6.

One could ask one selves, why not use a four point method? Basically two major arguments are against it. It is too clumsy a method to track sharp cusp like features. Basically the more points one uses the higher the order is of the polynomial one is fitting with. The measuring inaccuracy of the data points could cause miscellaneous higher order oscillation terms to be picked up which decrease the accuracy with which the derivative is determined. For our situation, a three measuring-point method turned out to be the optimum.

The whole procedure was automatized. The computer was told from which temperature to which temperature to scan, by which method the temperature should be increased (PID regulation or increasing the heater current), the size of the temperature or heater-current steps, the number of times an individual measurement had to be averaged to create a data point, the wanted accuracy in temperature and capacitance measurements etc.. This ensured the utmost of speed and consistency in the measurements. Files were generated containing the actual data and the relative length with its derivative (thermal expansion) versus temperature. With the use of

the local network this could be analyzed on a different computer while measurements were in process (so that alterations of settings could be performed if necessary).*

4.1 References

*temperature at which the derivative is determined

With the help of Eq. 4.19 and three measurements of the length for the sample at three different tempeature T_1,, T_2 and T_3 (denoted as $L(T_1)$, $L(T_2)$ and $L(T_3)$) the derivative of the length can be determined in a temperature, T, given as:

$$T := \%1^{1/3} + \frac{1}{36}\%2 + \frac{1}{6}\%3,$$

$$\begin{aligned}
\%1 := \frac{1}{216}(&-27\,T_3^4\,T_1\,T_2 + 21\,T_1^3\,T_2^3 - 51\,T_1^3\,T_3^3 - 15\,T_3^3\,T_2^3 + 18\,T_3^4\,T_2^2 \\
&+ 33\,T_3^5\,T_2 + 9\,T_2^5\,T_3 - 18\,T_3^2\,T_2^4 - 21\,T_2^5\,T_1 - 21\,T_3^5\,T_1 + 126\,T_1^4\,T_3^2 \\
&+ 36\,T_1^4\,T_2^2 - 63\,T_1^5\,T_2 - 99\,T_1^5\,T_3 + 18\,T_3^4\,T_1^2 - 15\,T_2^3\,T_3^2\,T_1 \\
&- 87\,T_3^3\,T_2^2\,T_1 + 225\,T_3^2\,T_2^2\,T_1^2 + 153\,T_2\,T_3^3\,T_1^2 - 183\,T_1^3\,T_2^2\,T_3 \\
&- 327\,T_1^3\,T_3^2\,T_2 + 9\,T_2^3\,T_1^2\,T_3 + 9\,T_2^4\,T_1\,T_3 + 243\,T_1^4\,T_3\,T_2 - 11\,T_3^6 \\
&+ 11\,T_2^6 + 27\,T_1^6)/(-T_2 + T_3)^3 + \frac{1}{108}(-1635\,T_3^7\,T_2\,T_1^2 + 723\,T_3^7\,T_1\,T_2^2 \\
&- 153\,T_2^9\,T_1 - 1968\,T_3^3\,T_2^3\,T_1^4 - 408\,T_3^3\,T_2^6\,T_1 + 75\,T_2^4\,T_1^6 - 765\,T_2^2\,T_1^8 \\
&+ 759\,T_2^3\,T_1^7 + 281\,T_1^9\,T_2 - 27\,T_1^{10} - T_2^{10} - 759\,T_3^4\,T_2^5\,T_1 - T_3^{10} \\
&- 36\,T_3\,T_2^8\,T_1 - 516\,x2^5\,T_1^5 - 24\,T_2^6\,T_1^4 + 331\,T_2^7\,T_1^3 + 3735\,T_3\,T_2^2\,T_1^7 \\
&- 742\,T_3\,T_2^6\,T_1^3 - 3312\,T_3\,T_2^3\,T_1^6 + 313\,T_3\,T_1^9 + 1482\,T_3^2\,T_2^6\,T_1^2 \\
&- 7392\,T_3^2\,T_2^2\,T_1^6 - 21\,T_3^2\,T_2^7\,T_1 + 4581\,T_3^2\,T_2\,T_1^7 + 864\,T_3^2\,T_2^4\,T_1^4 \\
&+ 4767\,T_3^2\,T_2^3\,T_1^5 - 3153\,T_3^2\,T_2^5\,T_1^3 + 33\,T_3\,T_2^4\,T_1^5 - 1755\,T_3\,T_1^8\,T_2 \\
&+ 1920\,T_3\,T_2^5\,T_1^4 - 309\,T_3\,T_2^7\,T_1^2 - 3008\,T_3^3\,T_2^4\,T_1^3 + 7797\,T_3^3\,T_2^2\,T_1^5 \\
&+ 2283\,T_3^3\,T_2^5\,T_1^2 - 6312\,T_3^4\,T_1^4\,T_2^2 - 106\,T_3^4\,T_1^3\,T_2^3 + 2943\,T_3^4\,T_2^4\,T_1^2 \\
&- 350\,T_3^4\,T_2^6 - 2013\,T_3^4\,T_1^6 + 35\,T_3^3\,T_2^7 + 1941\,T_3^3\,T_1^7 - 1125\,T_3^2\,T_1^8 \\
&- 24\,T_3^2\,T_2^8 + 160\,T_3\,T_2^9 + 6555\,T_3^4\,T_1^5\,T_2 - 783\,T_3^5\,T_2^3\,T_1^2 \\
&+ 5463\,T_3^5\,T_1^3\,T_2^2 - 5490\,T_3^5\,T_2\,T_1^4 - 1191\,T_3^5\,T_2^4\,T_1 + 3724\,T_3^6\,T_2\,T_1^3 \\
&+ 462\,T_3^6\,T_1\,T_2^3 - 3006\,T_3^6\,T_2^2\,T_1^2 + 242\,T_3^6\,T_2^4 - 146\,T_3^9\,T_2 \\
&+ 153\,T_3^9\,T_1 - 285\,T_3^8\,T_1^2 - 264\,T_3^8\,T_2^2 + 217\,T_3^7\,T_2^3 + 731\,T_3^7\,T_1^3 \\
&- 1464\,T_3^6\,T_1^4 + 1776\,T_3^5\,T_1^5 + 267\,T_3^5\,T_2^5 + 528\,T_3^8\,T_2\,T_1 \\
&- 6636\,T_3^3\,T_2\,T_1^6 + 39\,T_2^8\,T_1^2)^{1/2}\Big/(-T_2 + T_3)^2
\end{aligned}$$

$$\begin{aligned}
\%2 := (&5\,T_2^4 - 2\,T_2\,T_3^3 + 5\,T_3^4 - 14\,T_2\,T_1^3 - 22\,T_3\,T_1^3 + 2\,T_1\,T_2^3 - 2\,T_1\,T_3^3 \\
&+ 7\,T_3^2\,T_2^2 - 6\,T_3\,T_2^3 + 36\,T_3\,T_2\,T_1^2 + 3\,T_2^2\,T_1^2 + 15\,T_3^2\,T_1^2 \\
&- 12\,T_1\,T_2^2\,T_3 - 24\,T_1\,T_3^2\,T_2 + 9\,T_1^4)\Big/\Big((-T_2 + T_3)^2\,\%1^{1/3}\Big)
\end{aligned}$$

$$\%3 := \frac{-3\,T_3\,T_1 - T_2^2 + T_3^2 + 3\,T_1^2 + 3\,T_3\,T_2 - 3\,T_2\,T_1}{-T_2 + T_3}$$

1. A. de Visser, thesis, University of Amsterdam, 1986.
2. N. H. van Dijk, thesis, University of Amsterdam, 1994.
3. F. R. Kroeger and C.A. Swenson, J. Appl. Phys. 48, (1977) 853
4. K. van Hulst, J.A.A.J. Perenboom, IEEE-Trans. Magn., 24, (1988) 1397.
5. K. van Hulst, C.J.M. Aarts, A.R. de Vroomen and P. Wyder, J. Magn. Magn. Matt., 11 (1979), 317.
6. K. van Hulst and J.A.A.J. Perenboom Physica B, 164 (1990), 13.
7. N.F. Mott, Phil. Mag. 19 (1969) 835.
8. V. Ambegaokar, B.I. Halperin and J.S. Langer, Phys. Rev. B, 4 (1971) 2612.
9. R.W. Willekers, F Mathu, H.C. Meijer and H. Postman, Cryogenics 30 (1990 351.